

From Graphene Sheets to Boron Nitride Nanotubes via a Carbon-Thermal Substitution Reaction

Chun-Yin Ma, Ye-Yong Meng, Gui-Juan Shan, Li-Chao Sun, Shui-Chao Lin, Su-Yuan Xie,* Rong-Bin Huang, and Lan-Sun Zheng^[a]

Boron nitride nanotubes (BNNTs) are promising materials with unusual electronic,^[1] thermal,^[2] and mechanical properties,^[3] which are in many cases different from and/or superior to those of carbon nanotubes (CNTs).^[4] Among the widely discussed applications of BNNTs are their use as nanoscale semiconductors that can operate in oxidative environments at high temperatures^[2a] and as insulating composites with high thermal conductivity.^[2c,4] The methods for the synthesis of BNNTs include: arc discharge,^[5] laser ablation,^[6] carbon-thermal substitution,^[2a,7] chemical vapor deposition,^[8] and ball milling.^[9] In the carbon-thermal substitution reactions to synthesize BNNTs, CNTs have been used as morphology templates in which the carbon atoms of CNTs are substituted by boron and nitrogen atoms at high temperature.^[7] Experimental evidence has suggested that, for this carbon-thermal substitution reaction, the product morphologies are strictly template-dependent. For example, BNNT arrays,^[10a] activated BN,^[10b] and aluminum nitride nanowires^[10c] have been synthesized from their morphological carbon-template analogues. In contrast to this belief, herein we report a synthesis of tubular BNNTs starting from planar graphene sheets by a carbon-thermal substitution reaction. We present experimental evidence to demonstrate the morphologic transformation from planar sheets into tubular cylinders. Although the morphologic transformation from planar sheets into tubular cylinders has been supposed for a long time, experimental evidence for this transformation is still scarce. The growth of BNNTs from graphene

sheets in a carbon-thermal substitution reaction, which is apparently contradictory to the template-dependent carbon-thermal reactions described above, is not only useful for the macroscopic synthesis of BNNTs, but also informative for understanding the process of sheets scrolling.

Shown in Figure 1 are scanning electron microscopy (SEM), transmission electron microscopy (TEM), and atomic force microscopy (AFM) images for the graphene

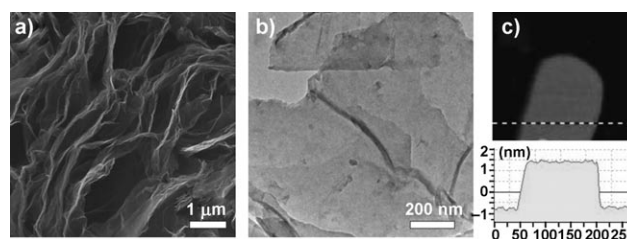


Figure 1. a) Typical SEM and b) TEM images of the graphene sheets. c) AFM image of a graphene sheet deposited on a mica substrate.

sheets which are employed in the present experiments (for detailed experimental procedures, see the Supporting Information). Their morphologies are planar, even at ambient conditions. Typical multilayered graphene sheets were employed with a topographic height of around 2 nm deposited on a mica substrate (Figure 1c). Figure 2 shows the SEM and TEM images of the products from the carbon-thermal reaction involving graphene sheets with H_3BO_3 and NH_3 .

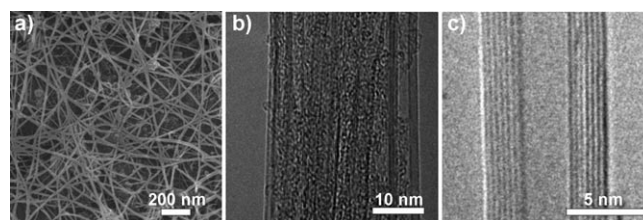


Figure 2. a) SEM and b) TEM images of the as-produced BNNTs. c) Typical HRTEM image of an as-produced BNNT.

[a] Dr. C.-Y. Ma, Y.-Y. Meng, G.-J. Shan, L.-C. Sun, S.-C. Lin, Prof. S.-Y. Xie, Prof. R.-B. Huang, Prof. L.-S. Zheng
State Key Laboratory of Physical Chemistry of Solid Surfaces & Department of Chemistry
College of Chemistry and Chemical Engineering
Xiamen University, 422 Si-Ming Road
Xiamen 361005 (China)
Fax: (+86) 592-2183047
E-mail: syxie@xmu.edu.cn

Supporting information for this article is available on the WWW under <http://dx.doi.org/10.1002/asia.201000839>.

The as-obtained one-dimensional (1D) materials, which were produced in high yield from the two-dimensional (2D) graphene sheets, are uniform and formed bunches. The bundled structure, as shown in Figure 2b, implies strong van der Waal interactions between the as-produced BNNTs and also a high-quality of the tubular structures. As confirmed by the high-resolution transmission electron microscopy (HRTEM; Figure 2c), the produced nanotubes are multi-walled with outer and inner diameters of approximately 7 and 3 nm, respectively. The distance between neighboring layers in the wall was circa 0.33–0.34 nm, which is in good agreement with the layer distance in multi-walled BNNTs synthesized previously.^[4] A small fraction of particles were also produced, but the amount of the particles could be reduced if starting from purified graphene sheets.

To further evaluate the quality of BNNTs synthesized from graphene sheets, X-ray photoelectron spectroscopy (XPS) measurements were conducted to analyze the B atom and N atom content in the BNNTs. The reactants, graphene sheets, were measured for comparison. Figure 3a shows the

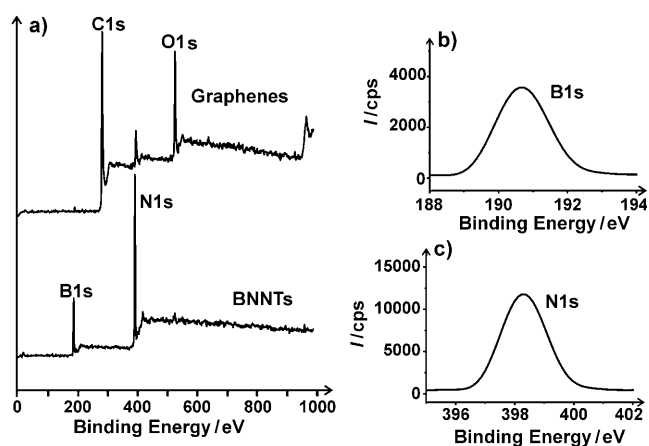


Figure 3. a) XPS spectra of the as-produced BNNTs and graphene reactants. b, c) Amplified XPS spectra of B1s and N1s for the as-produced BNNTs.

characteristic XPS spectrum of the graphene sheets, in which the N atom peak in addition to the C1s and O1s signals could be due to GO reduced by *para*-phenylene diamine (PPD). For the as-produced BNNTs, the composition can be established by the amplified XPS spectra of B1s and N1s at the binding energies of 190.6 and 398.2 eV, respectively (Figure 3b,c). The B/N ratio is about 1:1.03, which is approximately identical to the BN composition.

A Fourier transform infrared (FTIR) spectrum (Figure 4a) of the synthesized BNNTs revealed the characteristic peaks at around 1380 and 800 cm^{-1} , which were assigned to B–N vibrations parallel and perpendicular to the nanotube axis, respectively. The FTIR spectrum of the reactants of the graphene sheets modified by PPD (Figure 4a) showed a stretch for a benzene motif at 1579 cm^{-1} . The thermogravimetric analysis (TGA) of the BNNTs in air is shown in Figure 4b. It shows that the BNNTs are thermally stable

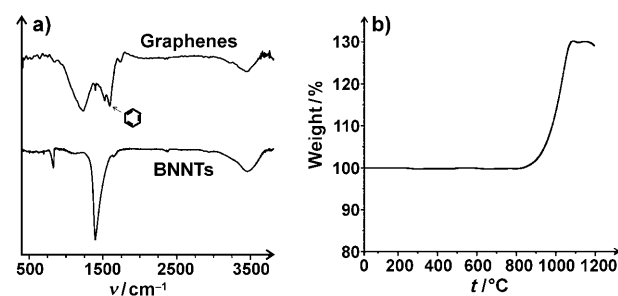
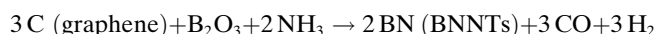


Figure 4. a) FTIR spectrum and b) TGA curve of the as-produced BNNTs. The FTIR spectrum of the graphene reactants is inset for comparison.

even at 940°C. The weight increase at higher temperatures is due to the oxidation of the BNNTs. The amount of increase (ca. 30%) is consistent with the estimated conversion from BN into B_2O_3 .

To corroborate the graphene-involving process in which the formation of BNNTs is involved in the substitution of graphene sheets, two other carbon sources (graphite oxide (GO) or carbon particles) were employed instead of graphene sheets as control experiments. When GO sheets were used (Figure 5a), the resultant products were still predominantly BNNTs but with poorer quality (Figure 5b–d). The outer diameters of the BNNTs, which typically had opened caps, were mainly in the range of 50–100 nm (Figure 5b,c), with typical interlayer distances of about 0.34 nm (Figure 5d). The wall thickness of the BNNTs was shown to be sensitive to the original layers of GO sheets involved. Quenching the reaction during the process of BNNTs growth afforded incomplete tubular structures with a wide range of diameters (Figure 5e). Figure 5f shows a TEM image of an intermediate structure, which was presumably formed from the scrolling of starting-reactant sheets and quenched at the termination of the growth. Accordingly, we conclude that the graphene sheets are involved in the formation of the BNNTs. Indeed, as shown in Figure 6, no tubular structure was produced when starting from carbon particles under the same carbon-thermal conditions.

As shown in Figure 7, sheet-like structures similar to the starting graphene sheets were produced in the absence of H_3BO_3 (or NH_3). However, the combination of both H_3BO_3 and NH_3 with graphene sheets produced 1D materials, rather than planar sheets. We assume a simultaneous process of both substitution reaction and curvature formation for the growth of the tubular structures as follows: B_2O_3 generated from H_3BO_3 powder is allowed to flow over the region containing the graphene sheets. The reaction involving graphene sheets, B_2O_3 , and NH_3 can be expressed as:



During the process in which the carbon atoms of the graphene sheets are substituted by boron and nitrogen atoms, the original planar structures of graphite with identical C–C

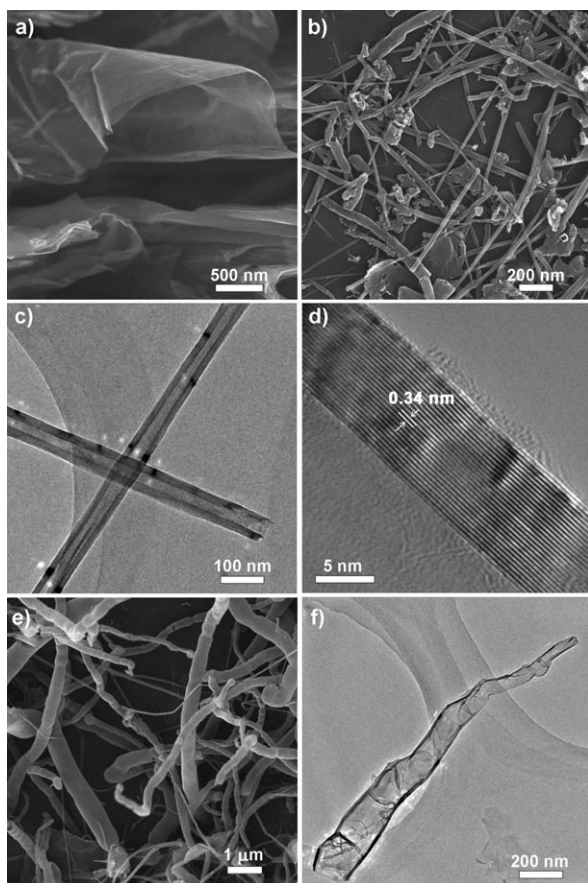


Figure 5. a) SEM image of the GO sheets (starting materials). b) SEM, c) TEM, and d) typical HRTEM images of the BNNTs produced from the GO sheets. e) SEM and f) TEM images of the intermediate structure(s) quenched in the BNNTs growth process.

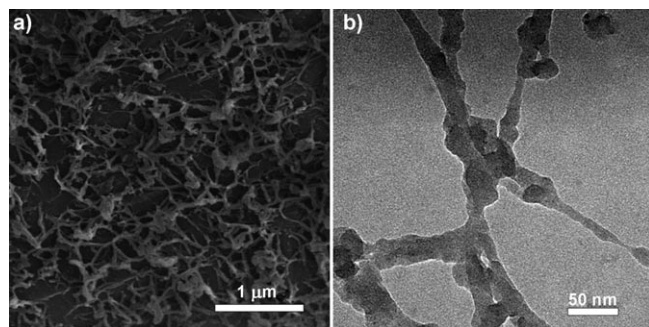


Figure 6. a) SEM and b) TEM images of the products synthesized from the carbon particles.

bond-lengths could be twisted and sequentially rolled up because of the incorporation of various C–B, C–N, and B–N bonds with diverse bond lengths. Moreover, the polarities of C–B, C–N, and B–N bonds might induce micro-electrostatic field that likely facilitates the formation of scrolled graphene sheets.^[11] In our experiment, if keeping the carbon-thermal reaction at the temperature of 1200 °C for a short time, nanoscrolls with multiple layers can be frequently seen. However, on annealing at the same temperature for a

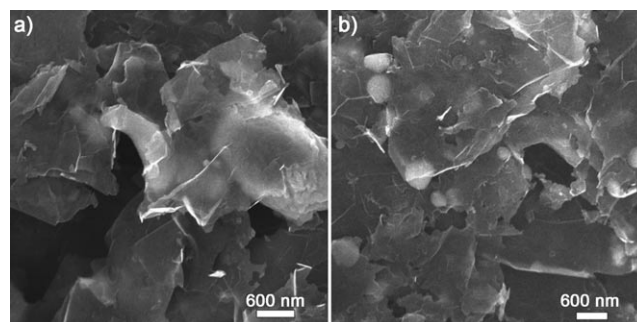


Figure 7. SEM images of the products synthesized from graphene sheets with a) boric acid or b) ammonia.

prolonged time, the intermediates of nanoscrolls could eventually structurally reform to BNNTs.

In conclusion, multi-walled BNNTs with outer diameters of around 7 nm and inner diameters of about 3 nm were unexpectedly grown from graphene sheets in a carbon-thermal substitution reaction involving B_2O_3 and NH_3 . This carbon-thermal process from planar graphene sheets to tubular BNNTs has both fundamental and practical importance, as: 1) the morphology transformation from sheets into nanotubes is different from the traditional dogma of the template-dependent carbon-thermal reaction; and 2) the availability of large amounts of BNNTs from graphene sheets provides opportunities for nanotechnological applications.

Experimental Section

To prepare graphene sheets, the graphite oxide (GO) was prepared by Hummers method using graphite ribbons as the starting reactant,^[12a] then mixed with a solution of PPD in *N,N*-dimethylformamide to obtain graphene sheets.^[12b] A mixture of graphene sheets (or GO sheets, carbon particles) with H_3BO_3 , was loaded into an alumina crucible, which was placed in a quartz tube (reactor) mouthed in a tubular furnace. Additional H_3BO_3 powder contained in another crucible was put in the upstream of the reactor (near the inlet of the quartz tube) to provide the boron source during the reaction. Ammonia was introduced as the source gas of nitrogen at a flow rate of 200 sccm under 1 atm pressure, whilst the furnace was heated up to 1200 °C for 5 h to complete the reaction. Argon was supplied as the protective/compensatory gas before and after the carbon-thermal substitution reaction. The raw product in the alumina crucible was further treated at 700 °C under the ambient condition for 12 h to get rid of the residual carbon. The morphology and structure of the produced BNNTs were characterized by scanning electron microscopy (SEM, Hitachi S4800), and transmission electron microscopy (TEM, TECNAI F-30). Atomic force microscopy (AFM) measurements were carried out in the tapping mode with an Agilent Instrument 5500ILM. X-ray photoelectron spectroscopy (XPS) was conducted using a PHI Quantum 2000 spectrometer. Thermogravimetric analysis (TGA) was taken on a SDT Q600, Fourier transform infrared (FTIR) spectra were recorded with a Nicolet AVATAR FT-IR360 spectrometer using the KBr pellet technique. For detailed experimental procedures, see the Supporting Information.^[13]

Acknowledgements

This work was supported by the NSFC (21031004, 21021061) and 973 Projects (2007CB815301, 2011CB935901). The present work was inspired

from the original synthesis of soluble BNNTs SXY performed in the group of Professor Ya-Ping Sun at Clemson University, USA.

Keywords: boron nitride nanotubes • carbon-thermal reactions • graphene sheets

- [1] a) A. Rubio, J. L. Corkill, M. L. Cohen, *Phys. Rev. B* **1994**, *49*, 5081; b) M. Radosavljević, J. Appenzeller, V. Derycke, R. Martel, Ph. Avouris, A. Loiseau, J.-L. Cochon, D. Pigache, *Appl. Phys. Lett.* **2003**, *82*, 4131; c) J. S. Lauret, R. Arenal, F. Ducastelle, A. Loiseau, M. Cau, B. Attal-Tretout, E. Rosencher, L. Goux-Capes, *Phys. Rev. Lett.* **2005**, *94*, 037405; d) W. Q. Han, H. G. Yu, C. Y. Zhi, J. B. Wang, Z. X. Liu, T. Sekiguchi, Y. Bando, *Nano Lett.* **2008**, *8*, 491; e) M. Ishigami, J. D. Sau, S. Aloni, M. L. Cohen, A. Zettl, *Phys. Rev. Lett.* **2005**, *94*, 056804.
- [2] a) W. Q. Han, W. Mickelson, J. Cumings, A. Zettl, *Appl. Phys. Lett.* **2002**, *81*, 1110; b) Y. Xiao, X. H. Yan, J. Xiang, Y. L. Mao, Y. Zhang, J. X. Cao, J. W. Ding, *Appl. Phys. Lett.* **2004**, *84*, 4626; c) T. Terao, Y. Bando, M. Mitome, C. Y. Zhi, C. C. Tang, D. Golberg, *J. Phys. Chem. C* **2009**, *113*, 13605; d) T. Terao, C. Y. Zhi, Y. Bando, M. Mitome, C. C. Tang, D. Golberg, *J. Phys. Chem. C* **2010**, *114*, 4340.
- [3] a) N. G. Chopra, A. Zettl, *Solid State Commun.* **1998**, *105*, 297; b) H. F. Bettinger, T. Dumitrică, G. E. Scuseria, B. I. Yakobson, *Phys. Rev. B* **2002**, *65*, 041406.
- [4] a) D. Golberg, Y. Bando, C. C. Tang, C. Y. Zhi, *Adv. Mater.* **2007**, *19*, 2413; b) C. Y. Zhi, Y. Bando, C. C. Tang, D. Golberg, *Mater. Sci. Eng. R* **2010**, *70*, 92.
- [5] a) N. G. Chopra, R. J. Luyken, K. Cherrey, V. H. Crespi, M. L. Cohen, S. G. Louie, A. Zettl, *Science* **1995**, *269*, 966; b) A. Loiseau, F. Willaime, N. Demoncy, G. Hug, H. Pascard, *Phys. Rev. Lett.* **1996**, *76*, 4737.
- [6] D. P. Yu, X. S. Sun, C. S. Lee, I. Bello, S. T. Lee, H. D. Gu, K. M. Leung, G. W. Zhou, Z. F. Dong, Z. Zhang, *Appl. Phys. Lett.* **1998**, *72*, 1966.
- [7] W. Q. Han, Y. Bando, K. Kurashima, T. Sato, *Appl. Phys. Lett.* **1998**, *73*, 3085.
- [8] a) O. R. Lourie, C. R. Jones, B. M. Bartlett, P. C. Gibbons, R. S. Ruoff, W. E. Buhro, *Chem. Mater.* **2000**, *12*, 1808; b) C. C. Tang, Y. Bando, T. Sato, K. Kurashima, *Chem. Commun.* **2002**, 1290; c) R. Z. Ma, Y. Bando, T. Sato, K. Kurashima, *Chem. Mater.* **2001**, *13*, 2965.
- [9] a) Y. Chen, J. F. Gerald, J. S. Williams, S. Bulcock, *Chem. Phys. Lett.* **1999**, *299*, 260; b) J. Yu, Y. Chen, R. Wuhler, Z. W. Liu, S. P. Ringer, *Chem. Mater.* **2005**, *17*, 5172.
- [10] a) F. L. Deepak, C. P. Vinod, K. Mukhopadhyay, A. Govindaraj, C. N. R. Rao, *Chem. Phys. Lett.* **2002**, 353, 345; b) W. Q. Han, R. Brutchey, T. D. Tilley, A. Zettl, *Nano Lett.* **2004**, *4*, 173; c) Y. J. Zhang, J. Liu, R. R. He, Q. Zhang, X. Z. Zhang, J. Zhu, *Chem. Mater.* **2001**, *13*, 3899.
- [11] A. Sidorov, D. Mudd, G. Sumanasekera, P. J. Ouseph, C. S. Jayanthi, S. Y. Wu, *Nanotechnology* **2009**, *20*, 055611.
- [12] a) W. S. Hummers, R. E. Offeman, *J. Am. Chem. Soc.* **1958**, *80*, 1339; b) Y. Chen, X. Zhang, P. Yu, Y. W. Ma, *Chem. Commun.* **2009**, 4527.
- [13] See the Supporting Information.

Received: November 25, 2010

Published online: March 17, 2011